Theoretical & Applied Mechanics Letters 6 (2016) 222–225

Contents lists available at ScienceDirect

Theoretical & Applied Mechanics Letters

journal homepage: www.elsevier.com/locate/taml

Letter

High temperature effects in moving shock reflection with protruding Mach stem

Xiaofeng Shi, Yujian Zhu *, Xisheng Luo, Jiming Yang

Advanced Propulsion Laboratory, Department of Modern Mechanics, University of Science and Technology of China, Hefei 230026, China

HIGHLIGHTS

- Protrusion of Mach stem is induced by a wall-jet behind it.
- High temperature effects intensify Mach stem protrusion.
- The mechanism is increase of energy buffer enhances wall-jet but weakens Mach stem.

ARTICLE INFO

Article history:
Received 31 May 2016
Received in revised form
12 July 2016
Accepted 7 August 2016
Available online 24 August 2016

Keywords:
Shock reflection
Numerical simulation
Protruding Mach stem
High temperature effects

ABSTRACT

The influence of high temperature effects on the protrusion of Mach stem in strong shock reflection over a wedge was numerically investigated. A two-dimensional inviscid solver applies finite volume method and unstructured quadrilateral grids were employed to simulate the flow. Theoretical analysis was also conducted to understand the phenomenon. Both numerical and theoretical results indicate a wall-jet penetrating forward is responsible for the occurrence of Mach stem protrusion. The protrusion degree seems to depend on the thermal energy buffer capacity of the testing gas. Approaches to increase the energy buffer capacity, such as vibrational relaxation, molecular dissociation, and increase of frozen heat capacity, all tend to escalate the protrusion effect.

Mach stem is normally treated as a straight shock perpendicular to the reflected wall in theoretical considerations of Mach reflection. It is however not always the case in reality. Protruding Mach stem has been experimentally discovered by many [1–4]. The protrusion not only makes the post-shock flow state deviate from the classical theoretical prediction, but also may fail the general transition criteria of reflection types. Recently, the phenomenon was also considered responsible for the shock bifurcation of cellular detonation wave [5,6]. The protrusion of Mach stem mainly occurs under the condition of strong incident shock and low specific heat ratio of gas [7]. By numerical simulation, Glaz et al. [8] discovered the wall jet-vortex rollup interaction structure which appears to integrate with the protruding Mach stem. Their results also implied that the thermochemical non-equilibrium effect tends to intensify the interaction and therefore to escalate the protrusion. Li and Ben-Dor [9] analyzed the interaction between wall-jet and Mach stem and proposed an analytical model to calculate the flow field associated with corresponding wave patterns. Detailed characteristics of the wall-jetting process were later numerically investigated by Vasilev et al. [10]. In the works of Li and Vasilev, nevertheless, the flow was considered thermo-chemically frozen and only mild Mach stem deformation was concerned. How the high temperature effect promotes Mach stem protrusion as well as the mechanism behind it has not yet been well understood. Therefore in this study, we carry out numerical tests on the Mach reflection of a strong moving shock over a wedge that has a protruding Mach stem, in which vibrational relaxation and chemical reactions are taking into account and their separate contributions are analyzed.

The numerical simulation is two-dimensional and inviscid. Dissociation chemistry and vibrational relaxation process of air molecules are built in with Gupta's 5-species chemical kinetic model [11] and Park's two-temperature model [12], respectively. The flow is simulated with finite volume method based on unstructured quadrilateral grids. Monotone upstream-centered schemes for conservation laws (MUSCL)-Hancock scheme [13] is employed to solve the parabolic part of the conservation equations, where the numerical fluxes are evaluated with a hybrid high level language (HLL)-high level language companion (HLLC) scheme [14]. The pure thermochemical sources are integrated with a mature ordinary differential equation (ODE) solver —

* Corresponding author.
E-mail address: yujianrd@ustc.edu.cn (Y. Zhu).

http://dx.doi.org/10.1016/j.taml.2016.08.006

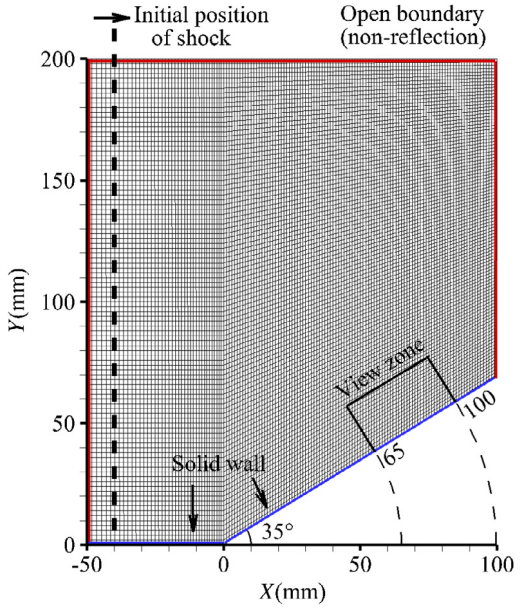

Fig. 1. Background grids and boundary conditions of the computational zone.

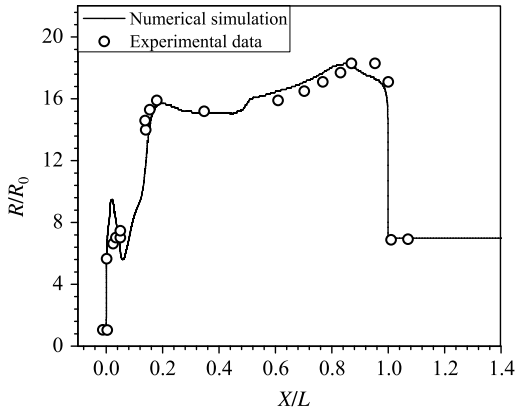

Fig. 2. Distribution of scaled density along the wedge surface.

"VODE", and join the parabolic part by fractional splitting method. Mesh adaptive technique is applied to accomplish a decent computational accuracy economically.

The computational zone and the initial grids are shown in Fig. 1. Floor and wedge surfaces are set as adiabatic slip walls, other boundaries are non-reflecting openings. The wedge angle is 35°. By 6 levels of adaptive mesh refinement, the grid size in regions of large density gradient may reach a minimum of 18 μm, i.e., 1/7000 of wedge length. The initial temperature and pressure of the undisturbed flow are 293 K and 0.05 atm, respectively. Taking a test case from Ref. [8] for code validation, as plotted in Fig. 2, it appears that the scaled density along the wedge surface between numerical result and experimental data agrees well.

High temperature effects were known to have significant influences on the flow [8]. To distinguish their particular influence, four gas models are tested, as listed in Table 1.

By varying the incident shock Mach number (M_s) and gas models, two types of typical flow patterns are observed. Representatives are shown in Figs. 3 and 4 (temperature contours). The view zone of the two figures is marked in Fig. 1. The basic wave systems of the two cases are both of double Mach reflection. Region (0) denotes the undisturbed flow. Region (1) denotes the flow behind the incident shock. Region (2) and region (3) are the flows behind the primary reflected shock (T–T′) and the primary Mach stem (T–G),

Table 1
Gas models.

No.	Gas models	Dissociation
1	Frozen	Off
2	Thermal non-equilibrium	Off
3	Thermal equilibrium	Off
4	Thermochemical non-equilibrium	On

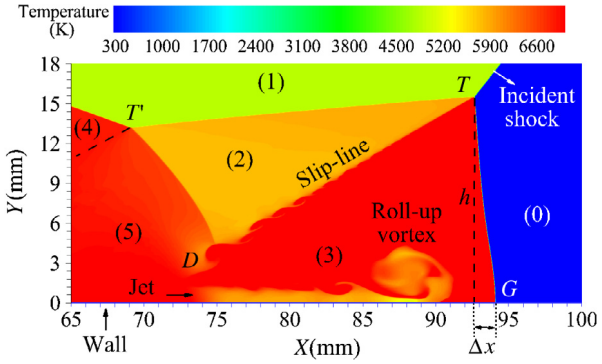

Fig. 3. Temperature contours of a DM-WR flow (M_s 9, θ_w 35°, frozen flow).

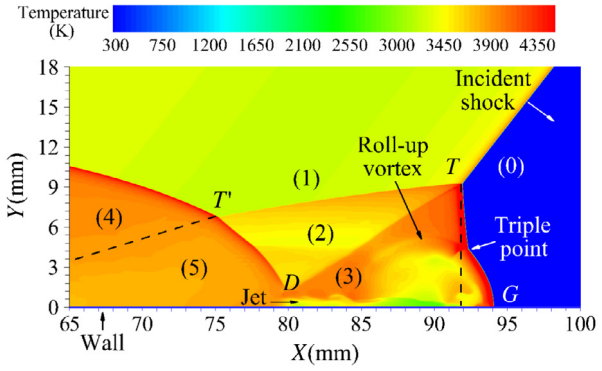

Fig. 4. Temperature contours of a TM-WR flow (M_s 9, θ_w 35°, thermochemical non-equilibrium flow).

which are separated by a slip line (T–D). And region (5) and region (4) are the flows behind the secondary reflected shock (T′–D) and Mach stem.

The two reflection types share a few common features. First, a jet is generated around the intersection of slip line and wedge surface. The jet shoots forward along the surface and finally rolls up to form a vortex. Second, disturbed by the vortex, the lower part of the Mach stem protrudes as an arc, with the root of it keeping perpendicular to the reflecting wall. The difference mainly lies in the connection between the protruding part of the Mach stem and the rest. Figure 3 presents a whole piece of smoothly curved Mach stem with no obvious conjunction, while in Fig. 4 a new triple point is formed in the middle. Following the definition of Semenov [4], the former reflection is referred as double Mach–White reflection (DM-WR) and the latter as triple Mach–White reflection (TM-WR).

A non-dimensional parameter

$$f = \frac{\Delta x}{h} \tag{1}$$

is defined to characterize the protruding extent of the Mach stem, where h denotes the height of the Mach stem and Δx the distance between theoretical and practical pedals of the Mach stem.

The protrusion parameter f resulting from four different gas models are shown in Fig. 5 for comparison. It is found that the boundary between DM-WR and TM-WR can be well depicted by a

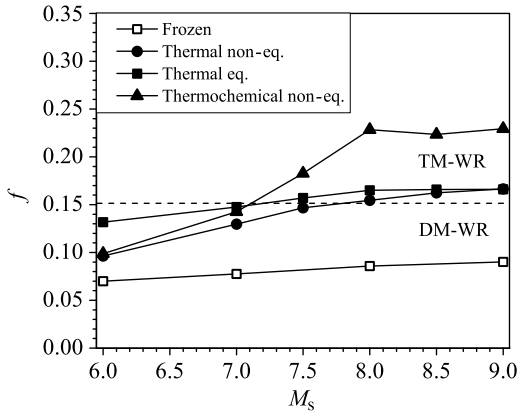

Fig. 5. Non-dimensional deformation of Mach stem along with incident shock Mach number.

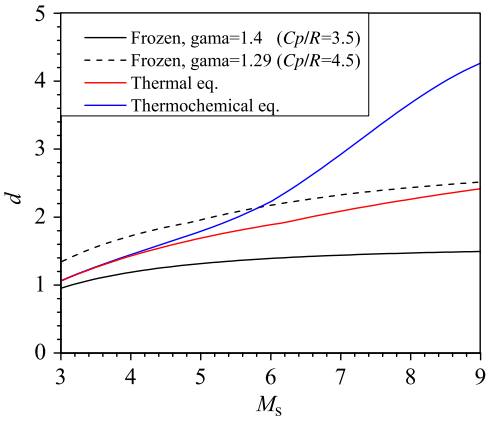

Fig. 6. Jet intensity along with the shock Mach number in different gamma and equilibrium state conditions.

single f within the current testing range. That is, TM-WR generally happens when f exceeds 0.15, no matter what the gas model is.

Gas models 1–3 consider only the difference of vibrational relaxation, but not dissociation. Clearly, thermal equilibrium flow always leads to a larger f than frozen flow. The protruding extent almost doubles. For thermal non-equilibrium flow, as expected, the deformation degree is between those of frozen and thermal equilibrium. When the incident shock Mach number is small, the Mach stem protrusion in thermal non-equilibrium flow is close to that in frozen flow. With the increase of shock Mach number, it approaches gradually towards the thermal equilibrium case. This is because the vibrational relaxation speed rises with the temperature, and the gas behind a weaker shock wave takes longer time to reach thermal equilibrium state, which is therefore more likely to remain partially frozen when passing through the reflection wave system.

Gas model 4 activates chemical reaction upon the basis of gas model 2. As well, the chemical reaction intensifies the protrusion of Mach stem. This effect becomes remarkable as the incident shock Mach number goes higher than 7, for this is where dissociation begins to massively occur behind the Mach stem and a considerable amount of atoms (first oxygen then nitrogen) will be produced afterward. The reason of dissociation escalating Mach stem protrusion is to be explained later. At shock Mach number 8, the effect of dissociation seems to reach a maximum, after which the protrusion parameter f suddenly levels. Overall, the results indicate that the contribution of dissociation in Mach stem protrusion can be comparable to that of thermal relaxation.

Given the complexity of the jet and vortex flow behind the Mach stem, it is hard to predict the exact protruding extent. However, the qualitative effect of protrusion and the dependence of it may be estimated through certain calculations [9]. The wall-jet is essentially driven by the pressure difference between regions (3) and (5) (Figs. 3 and 4). Assuming isentropic jet, the velocity of the jet flow relative to point D, V_{jet}, can be easily deduced. On the other hand, the Mach stem keeps drifting away from point D with a knowable velocity, V_{DG}. The theoretical protrusion degree then can be expressed as the overriding degree of the jet,

$$f_c = \frac{\Delta x}{h} = \frac{\Delta x}{\alpha \cdot x_{\text{DG}}} = \frac{V_{\text{jet}} - V_{\text{DG}}}{\alpha \cdot V_{\text{DG}}} \tag{2}$$

with α a constant geometrical coefficient. The larger the value of f_c is, the stronger the Mach stem protrusion is expected to be. Dismissing α, we introduce a theoretical protrusion factor

$$d = \frac{V_{\text{jet}} - V_{\text{DG}}}{V_{\text{DG}}}. \tag{3}$$

Figure 6 shows the d curves calculated with different gas models. Because the momentum dissipation of jet and vortex is not considered in above derivation, the theoretical results significantly overestimate the protrusion extent. Despite that, the relativity and the variation trend of d turn out to be in good agreement with the numerical results of f in Fig. 5. This confirms the mechanism of high temperature effects on the Mach stem protrusion lies in the fundamental fluid dynamics associated with the thermodynamic properties of gas.

The reason for the phenomenon is rather clear. The extra energy absorption of vibrational relaxation and molecular dissociation tend to weaken the strength of Mach stem. As a reversed process, the release of the extra vibrational energy and chemical energy stored in high temperature region (5) tends to induce a stronger jet in region (3). Under the same mechanism, simply increasing the heat capacity of gas should lead to a similar consequence. To demonstrate that, d for a higher frozen Cp (gamma $=$ 1.29) is calculated and plotted in Fig. 6. It shows that higher heat capacity indeed causes a larger protruding extent.

In summary, a numerical investigation of high temperature effects on Mach stem protruding phenomenon is carried out. Numerical results and theoretical analysis exhibit direct links between the wall-jet and the protrusion of Mach stem. High temperature effects including vibrational relaxation and molecular dissociation tend to escalate the protrusion. Increase of heat capacity favors protrusion as well. The mechanism behind them is essentially the same. There is a strength competition between two opposite processes—the Mach stem compression and the wall-jet expansion. The balance between them seems to greatly depend on the buffer capacity of thermal energy. The larger the buffer capacity is, the weaker the compression and the stronger the expansion will be, and therefore the more severely the Mach stem will be disturbed by the jet.

References

[1] S. Ando, Pseudo-stationary oblique shock-wave reflection in carbon dioxide — domains and boundaries, Technical Report, UTIAS Technical Note No. 231, 1981.
[2] J. Lee, I. Glass, Domains and boundaries of pseudo-stationary oblique shock-wave reflection in air, Technical Report, UTIAS Technical Note No. 262, 1982.
[3] J. Foster, P. Rosen, B. Wilde, et al., Mach reflection in warm dense plasma, Phys. Plasmas 17 (2010) 112704.
[4] A. Semenov, M. Berezkina, I. Krassovskaya, Classification of pseudo-steady shock wave reflection types, Shock Waves 22 (2012) 307–316.
[5] P. Mach, M. Radulescu, Mach reflection bifurcations as a mechanism of cell multiplication in gaseous detonations, Proc. Combust. Inst. 33 (2011) 2279–2285.

[6] L. Maley, R. Bhattacharjee, S. Lau-Chapdelaine, et al., Influence of hydrodynamic instabilities on the propagation mechanism of fast flames, Proc. Combust. Inst. 35 (2015) 2117–2126.
[7] I. Glass, Some aspects of shock-wave research, AIAA J. 25 (1987) 214–229.
[8] H. Glaz, P. Colella, J. Collns, et al., Nonequilibrium effects in oblique shock-wave reflection, AIAA J. 26 (1988) 698–705.
[9] H. Li, G. Ben-Dor, Analysis of double-mach-reflection wave configurations with convexly curved mach stems, Shock Waves 9 (1999) 319–326.
[10] E. Vasilev, G. Ben-Dor, T. Elperin, et al., The wall-jetting effect in mach reflection: Navier–Stokes simulations, J. Fluid Mech. 511 (2004) 363–379.
[11] R. Gupta, J. Yos, R. Thomopson, et al., A review of reaction rates and thermodynamic and transport properties for an 11-species air model for chemical and thermal nonequilibrium calculations to 30000 k, Technical Report, AIAA, 1985.
[12] C. Park, On convergence of computation of chemically reacting flows, Technical Report, AIAA, 1985.
[13] E.F. Toro, Riemann Solvers and Numerical Methods for Fluid Dynamics, Spring Press, 1997.
[14] H. Nishikawa, K. Kitamura, Very simple, carbuncle-free, boundary-layer-resolving, rotated-hybrid riemann solvers, J. Comput. Phys. 227 (2008) 2560–2581.